Mitotic Activation Around Wound Edges and Epithelialization Repair in UVB-Induced Capsular Cataracts

Zongbo Wei,[1] Caili Hao,[1] Ramkumar Srinivasagan,[2] Hongli Wu,[3,4] Jian-Kang Chen,[1] and Xingjun Fan[1]

[1]Department of Cellular Biology and Anatomy, Medical College of Georgia at Augusta University, Augusta, Georgia, United States
[2]Department of Pharmacology, Case Western Reserve University, Cleveland, Ohio, United States
[3]Pharmaceutical Sciences, College of Pharmacy, University of North Texas Health Science Center, Fort Worth, Texas, United States
[4]North Texas Eye Research Institute, Pharmaceutical Sciences, University of North Texas Health Science Center, Fort Worth, Texas, United States

Correspondence: Xingjun Fan, Department of Cellular Biology and Anatomy, Medical College of Georgia at Augusta University, 1460 Laney Walker Boulevard, CB Building, Room CB1119, Augusta, GA 30912, USA; xfan@augusta.edu.

Received: June 14, 2021
Accepted: December 8, 2021
Published: December 30, 2021

Citation: Wei Z, Hao C, Srinivasagan R, Wu H, Chen JK, Fan X. Mitotic activation around wound edges and epithelialization repair in UVB-induced capsular cataracts. *Invest Ophthalmol Vis Sci.* 2021;62(15):29. https://doi.org/10.1167/iovs.62.15.29

Purpose. Ultraviolet B (UVB) has been well documented to induce capsular cataracts; however, the mechanism of the lens epithelial cell–mediated repair process after UVB irradiation is not fully understood. The purpose of this study was to better understand lens epithelial cell repair after UVB-induced epithelium damage.

Method. C57BL/6J mice were irradiated by various doses of UVB. Lens morphology and lens capsule opacity were monitored by slit lamp, darkfield microscopy, and phase-contrast microscopy. Lens epithelial cell mitotic activation and cell apoptosis were measured by immunohistochemistry. Lens epithelial ultrastructure was analyzed by transmission electron microscopy.

Results. UVB irradiation above a dose of 2.87 kJ/m^2 triggered lens epithelial cell apoptosis and subcapsular cataract formation, with a ring-shaped structure composed of multilayered epithelial cell clusters manifesting a dense ring-shaped capsular cataract. The epithelial cells immediately outside the edge of the ring-shaped aggregates transitioned to mitotically active cells and performed wound healing through the epithelialization process. However, repairs ceased when lens epithelial cells made direct contact, and scar-like tissue in the center of the anterior capsule remained even by 6 months after UVB irradiation.

Conclusions. Our present study demonstrates that normally quiescent lens epithelial cells can be reactivated for epithelialization repair in response to UV-induced damage.

Keywords: lens opacity, ultraviolet light, UVB, epithelialization, lens epithelium

Age-related cataracts are consequences of accumulated damage to lens proteins, lipids, and DNA by multiple contributing factors. Because of constant exposure to sunlight, accumulated ultraviolet (UV)-mediated lens damage has long been considered as one of the primary risk factors for age-related cataracts, well supported by numerous case and epidemiological studies.[1–6] According to the Chesapeake Bay eye study,[7] an epidemiologic survey of 838 watermen who had constant UV exposure working in the Chesapeake Bay area, there is an strong association between exposure to UVB radiation and cataract formation. A doubling of cumulative UV exposure increased the risk of cortical cataract development by a factor of 1.60. A similar increased risk of acquiring cataracts in areas of higher UV irradiation was reported in an Australian Aborigine study with a cohort of 64,307 participants.[8] Recently, Miyashita et al.[9] performed a cross-sectional study to survey the level of UV exposure and prevalence of cataract formation and concluded that increased cumulative ocular UV exposure might carry a high risk for developing nuclear cataracts, posterior subcapsular cataracts, retrodots, and ring-shaped cortical cataracts. Moreover, Yu et al.[10] surveyed participating individuals living at two different altitudes with an almost 4000-m gap and found that the individuals living at the high altitudes with high UV exposure had a significantly higher risk of developing lens opacity than those living at low altitudes with lower UV exposure.

Both UVA (315–400 nm) and UVB (280–315 nm) can cause damage to the lens. As compared with UVA, UVB has relatively higher energy and may induce more severe cellular DNA damage of the lens epithelial cells (LECs) of bovines,[11] rabbits,[12,13] mice,[14] and humans.[15] Other than its well-documented DNA damaging effects, UV irradiation also causes protein damage in the lens. For example, UVB can

induce both β- and γ- crystallin aggregation.[16] Similarly, UVA promotes deamidated αB crystallin dimerization and degradation[17] and also decreases the α crystallin chaperone-like function in an age-related manner.[18] Furthermore, UVB has been found to negatively alter several metabolism-associated enzymes, including hexokinase, phosphofructokinase, and isocitrate dehydrogenase, particularly in the aged lenses.[19]

A healthy lens is able to absorb almost all UV radiation by various UV filters, including small tryptophan metabolites, such as 3-hydroxykynurenine, *O*-β-D-glucoside (3OHKG) and kynurenine, and protein-bound tryptophan residues.[20] However, the major free UV filters (i.e., 3OHKG and kynurenine) decrease linearly with age, impairing the capacity of the lens to block photooxidation.[21] In contrast, protein-bound kynurenine steadily increases with age in human lenses, and protein-bound kynurenine has been found to facilitate lens protein oxidative damage via singlet-oxygen mediated photooxidation.[22] Furthermore, the age-related accumulation of advanced glycation endproducts (AGEs) also serves as UV sensitizers that can facilitate UV-mediated generation of reactive oxygen species.[23,24] Linetsky et al.[25] found that UVA could excite kynurenines in both free and protein-bound forms to oxidize ascorbic acid (vitamin C). Ascorbic acid oxidation and lens crystallin modification by ascorbylation have been found to be closely associated with age-related cataractogenesis.[26,27]

UV-induced animal cataract models have been successfully established and broadly used in studying lens photooxidation,[28] DNA damage and repair,[11,15] gene expression,[29] protein aggregation,[30] lens morphology and optics,[31] metabolisms,[32] and cataractogenesis.[33,34] Meyer et al.[33] found that C57BL/6 mice developed an annular ring–style subcapsular cataract after a 5-kJ/m^2 dose of UVB irradiation, with the size of the annulus gradually decreasing with time. Zhang et al.[35] found that aged mice were more susceptible to UVB-induced subcapsular cataracts compared with young mice because young mice were able to effectively upregulate thiol-repair enzymes such as thioltransferase and thioredoxin. Interestingly, a rapid capsular self-repair phenomenon was consistently noticed in these UVB-induced mouse subcapsular cataract studies; however, the mechanism of the lens epithelial repair process remains largely unknown. To answer this important question, we also established an in-house UVB irradiation system in our lab. The rapid annular ring closure and the final unrepaired scar-like tissue inspired us to explore the possible mechanisms of lens epithelial cell repair after UVB-induced damage. In the present study, we discovered that the generally quiescent epithelial cells at the lens anterior central zone could be reactivated in response to UVB and to repair the lens epithelium damage via the epithelialization process. Our findings may provide new insights into lens self-repair processes.

Methods

Reagents

All chemicals used were of analytical reagent grade. Milli-Q water was used for the preparation of standards and reagents. Bromodeoxyuridine (BrdU; B23151), 4′,6-diamidino-2-phenylindole (DAPI; P36931), and Hoechst 33342 (H3570) were purchased from Thermo Fisher Scientific (Waltham, MA, USA). Pro-caspase 3 (MA1-91637), BrdU (BU-1), and glyceraldehyde-3-phosphate dehydrogenase (GAPDH; PA1-987) antibodies were also purchased from Thermo Fisher Scientific. Cleaved caspase 3 antibody (9664) was purchased from Cell Signaling Technology (Danvers, MA, USA). Apurinic/apyrimidinic endonuclease 1 (APE1; Sc-17774) used for immunofluorescence staining and APE1 (Sc-55498) used for immunoblot were purchased from Santa Cruz Biotechnology (Dallas, TX, USA). Anti-β5 integrin antibody (LS-C332121) was purchased from LSBio (Seattle, WA, USA). β-Actin antibody (4970) was purchased from Cell Signaling Technology. All other chemicals were obtained from Sigma-Aldrich (St. Louis, MO, USA) and Thermo Fisher Scientific.

Cell Culture and Treatment

The mouse lens epithelial cell line, 17EM15, was provided by Salil Lachke, PhD, at the University of Delaware. 17EM15 cells were grown in Dulbecco's Modified Eagle's Medium with 10% fetal bovine serum, 2 mmol/L glutamine, and 50 U/mL penicillin/streptomycin (HyClone; Cytiva, Marlborough, MA, USA) at 37°C in a humidified 5% CO_2 incubator. Then, 5×10^5 cells/dish were seeded 16 hours before treatment in a 60-mm culture dish. Cells were treated by a freshly prepared full medium containing 0 and 1 µM staurosporine (STS), an established trigger for apoptosis. Cells were harvested at 7 hours for analysis.

Animals

All animal experiments were performed in accordance with procedures approved by the Augusta University Animal Care and Use Committee and conformed to the ARVO Statement for the Use of Animals in Ophthalmic and Vision Research. C57BL/6J mice (000664) were purchased from The Jackson Laboratory (Bar Harbor, ME, USA) and housed under a diurnal lighting condition with allowance to free access to food and water. Three-month-old mice were used for UVB irradiation.

UVB System and Animal Exposure

We made an in-house UVB system following the study by Zhang et al.,[35] with an additional power output adjustable function. The UVP XX-15MR UV lamp (Analytik Jena, Upland, CA, USA) contains a double parallel 302-nm 15-W tube that is used as the UVB source. The UVB power output was adjusted by changing the height of the UV lamp. The actual UVB exposure was measured using a digital UVX radiometer with a UVX-31 302-nm sensor (Analytik Jena). A correction factor of 1.43 provided by Analytik Jena was used to calculate the final UVB dose.

The UVB system was warmed up for at least 5 minutes before the animal exposure experiment started. Mydriatic eye drops (1% atropine) were topically applied followed by anesthetizing with a diluted xylazine and ketamine cocktail. Mice were placed at the exact level of the UVX-31 sensor (30–60 cm adjustable distance from UV source to mice) and exposed once and for a specific time defined by the desired power output.

Lens Opacity Analysis by Slit Lamp, Darkfield Microscopy, and Phase-Contrast Microscopy

The lens opacity was first documented by a slit lamp (SL-D4; Topcon, Livermore, CA, USA) with 40× magnification every day for the first 12 days after UVB irradiation and then every 2 weeks. The mydriatic eye drop (0.5% tropi-

Investigative Ophthalmology & Visual Science

camide ophthalmic solution; NDC 1748-101-12; Akorn, Lake Forest, IL, USA) was given 5 minutes before the slit-lamp recording. Mice were anesthetized by isoflurane (46066-755-04; Aspen Veterinary Resources, Liberty, MO, USA) during the procedure. At the end of each experimental time point, the mice lenses were dissected and a darkfield image was taken with a Leica M80 microscope (Leica, Buffalo Grove, IL). Lastly, the lens capsule was dissected, and the capsular opacity was documented by a Leica M80 microscope and a Leica DMi1 phase-contrast microscope (Leica Microsystems, Wetzlar, Germany).

Capsular Cataract Quantification

The area (mm^2) of the capsular cataract was quantitatively measured by ImageJ software (National Institutes of Health, Bethesda, MD, USA), and values were expressed as mean ± standard deviation.

Capsule Dissection and Immunofluorescence Staining

The lens capsule was dissected as described in our previous study[36] but avoiding a deep cut into the anterior region to keep the entire germinative zone and anterior capsule intact. The dissected capsules were fixed immediately with 4% paraformaldehyde (PFA) containing 1 µg/mL Hoechst 33342 at room temperature (RT) for 15 minutes. The fixed capsules were rinsed two times with PBS for 5 minutes each time before being permeabilized by 0.5% Triton X-100 for 15 minutes at RT. For membrane protein β5 integrin staining, no membrane permeabilization was performed. Nonspecific targets were blocked by 5.0% goat serum for 30 minutes at RT and then stained with an anti-Ki67 antibody (1:200, 151204; BioLegend, San Diego, CA, USA), anti-cleaved caspase 3 antibody (1:200, 9664; Cell Signaling Technology), anti-APE1 antibody (1:100, sc-17774; Santa Cruz Biotechnology), anti-β5 integrin antibody (1:100, LS-C332121; LifeSpan Biosciences, Seattle, WA, USA), and Alexa Fluor 488 Phalloidin (1:200, A12379; Thermo Fisher Scientific) overnight at 4°C. Following the primary antibody incubation, capsules were washed three times (5 minutes each) with PBS plus 0.1% Tween 20 (PBST) before being incubated with the proper secondary antibody conjugated with fluorescent dye at RT for 1 hour. Capsules were then mounted with mounting medium (23002; Biotium, Fremont, CA, USA) for image capture.

BrdU Labeling

Mice with or without UVB irradiation were given 2 mg BrdU each via intraperitoneal administration. Twenty-four hours after the injection, the mice were euthanized, and the lenses were collected. Each lens capsule was dissected and fixed immediately with 4% PFA containing 1 µg/mL Hoechst 33342 at room temperature for 15 minutes. The capsule was washed twice (5 minutes each) with PBS before being incubated in 2N hydrochloric acid (HCL) in PBST at room temperature for 30 minutes. After the two PBS washes (5 minutes each), each capsule was permeabilized with 0.5% Triton X-100 for 15 minutes. Subsequently, the capsule was blocked by 5.0% goat serum for 30 minutes before incubation with BrdU antibody (1:300 dilution) for 14 hours at 4°C. Then, the capsule was washed another three times with PBST (5 minutes each), and Alexa Fluor 488 conjugated secondary antibody was then applied for 1 hour at RT. Each capsule was again washed three times (5 minutes each) with PBS and mounted with mounting medium (Biotium) for image capture.

Immunofluoresent Staining of Paraffin Sections

After deparaffination and rehydration by xylene and gradient ethanol, respectively, antigen retrieval was performed by immersing the sections in sodium citrate buffer (10-mM sodium citrate and 0.05% Tween 20, pH 6.0) or TE buffer (10-mM Tris base, 1-mM EDTA solution, and 0.05% Tween 20, pH 9.0) in a hot steamer instrument for 20 minutes. Following retrieval, each slide was cooled down for 10 minutes at room temperature before being rinsed two times (5 minutes each) with PBS. Membrane permeabilization was achieved by incubating with 0.5% Triton X-100 for 10 minutes at RT. The non-specific background was blocked by 5.0% goat serum for 30 minutes at RT and then stained with an anti–α-smooth muscle actin (SMA) antibody (1:500, F3777; Sigma-Aldrich), anti-vimentin antibody (1:1000, PA5-27231; Thermo Fisher Scientific), and anti-fibronectin antibody (1:200, ab268020; Abcam, Cambridge, UK) at 4°C overnight. The next day, sections were washed three times (5 minutes each) with PBST before being incubated with the proper secondary antibody conjugated with fluorescent dye at RT for 1 hour. After three washings (5 minutes each) with PBST, the sections were mounted with mounting medium and ready for image capture.

Transmission Electron Microscopy

Lens capsules were fixed by 2% glutaraldehyde in 0.1-M sodium cacodylate buffer, pH 7.4, for 24 hours at RT and then subjected to transmission electron microscopy (TEM) analysis using the JEM-1400Flash TEM system (Jeol USA, Peabody, MA, USA).

Confocal Microscopy

All images were captured using a Leica STELLARIS confocal microscopy and were analyzed with LAS X software.

Immunoblot Assays

Immunoblot assays were performed as previously described.[37] In brief, the protein concentration from the supernatant was measured by protein bicinchoninic acid assay (Thermo Fisher Scientific). Equal amounts of protein were subjected to appropriate sodium dodecyl sulfate–polyacrylamide gel electrophoresis gel electrophoresis and transferred to a 0.45-µm pore size polyvinylidene fluoride membrane. Detection was done using the ECL western blotting detection system.

Results

UVB Induces Anterior Capsular Opacity, Leading to Formation of a Multiple Cell Layer Ring-Shaped Structure

After monitoring capsular opacification from different doses of UVB irradiation, we noticed that 4 days after UVB irradiation mice displayed the most striking capsular opacity.

Investigative Ophthalmology & Visual Science

As shown in Figure 1B, a large ring-shaped structured opacity was observed 4 days after 24.7-kJ/m^2 of UVB irradiation in comparison with unexposed control lenses (Fig. 1A). A less dense opacity was also seen inside the ring in the center of the anterior capsule (Fig. 1B). To confirm the capsular opacity, we separated the lens capsule from the lens. As illustrated in Figure 1D, capsular opacity and dense ring-shaped structures were clearly seen in UVB irradiated mouse lenses compared with unexposed lenses (Fig. 1C).

To better understand the ring-shaped structure, we stained the lens capsule whole mount with an F-actin antibody. The three-dimensional projection illustrated in Figures 1E to 1G demonstrated that the ring-shaped structure was formed by a multilayer of irregularly stacked lens epithelial cells, which manifested as a dense opacity. To further confirm our findings, we also carried out a TEM study. As shown in Figures 1H and 1I, irregularly stacked cells were seen clustering around the edges of the UVB-exposed zone (Fig. 1J).

UVB Induces Lens Epithelial Cell Apoptosis

UVB can induce DNA damage and cell apoptosis; it has been shown to induce LECs apoptosis from the *in vitro* LECs culture and *in vivo* rat irradiation studies.[14,38] To measure LEC apoptosis in the lens epithelium impacted by UVB, we monitored caspase 3 activation via immunofluorescence staining of the lens capsule whole mount with a cleaved caspase 3 antibody. As shown in Figures 2G and 2H, massive numbers of cleaved caspase 3–positive lens epithelial cells were detected within the ring-shaped zone in response to the 24.7-kJ/m^2 UVB irradiation, suggesting that active LEC apoptosis is caused by UVB-mediated damage. No cleaved caspase 3-positive cells were detected outside the UVB-damaged zone or in the capsules without UVB irradiation (Figs. 2A, 2B). The highly magnified images of selected regions from Figures 2A to 2C are illustrated in Figures 2D to 2F, and images from Figures 2G to 2I are shown in Figures 2J to 2L. We also confirmed the caspase 3 activation by measuring cleaved caspase 3 using immunoblot analysis. As shown in Figure 2M, cleaved caspase 3 was detected in the UVB irradiated mouse lens capsule. A detectable, yet not striking, cleaved caspase 3 band from the total capsular lysate was expected because only LECs from the UVB impact zone underwent apoptosis. Of note, in order to obtain a full image of the lens capsule with an intact lens germinative zone and anterior capsule, we isolated the lens capsule by a small incision at the posterior capsule. The partial lens posterior capsule was folded along the edges of the germinative lens zone, so some non-specific fluorescence signals were trapped and seen at the edge of the lens capsular whole mount after z-stack projection.

Lens Epithelial Cells Initiate a Rapid But Incomplete Repair Via an Epithelialization Process

In an effort to establish the time course of a UVB-induced mouse capsular cataract model, we noticed a rapid lens capsule repair phenomenon from day 4 to day 8 (Figs. 3A, 3B), similar to that previously reported for UVB-induced mouse models.[35,39] As shown in Figure 3D, 4 days after UVB irradiation the ring-shaped structure displayed a dense opacification, and disorganized epithelial cells were also observed within the ring of the UVB-affected regions. In contrast, a nicely intact lens epithelial cell layer was seen outside the UVB-exposed zone (repaired zone). The rapid repair process replaced the damaged lens epithelium with a newly synthesized epithelial cell layer (Figs. 3D, 3E), referred to as an epithelialization process. Notably, the repaired areas of the capsule demonstrated normal lens epithelium alignment with a transparent morphology. However, this rapid repair slowed down significantly after day 8, and afterward we still observed a scar-like opacity in the center of the anterior capsule (Fig. 3E). All five experimental animals produced similar images of cataracts formation on day 4 and the rapid repair within 6 days after UVB irradiation (Supplementary Fig. S1).

UVB irradiation has been well known to cause direct DNA damage by, for example, inducing photolesions, including pyrimidine (6–4) pyrimidone photoproducts (6–4PPs) and cyclobutane pyrimidine dimers.[14,40,41] To cope with the DNA damage, cells have developed several repair mechanisms. In these repair pathways, the base excision repair (BER) and nuclear excision repair (NER) are the two dominant mechanisms responsible for repairing UVB-induced DNA damage.[42,43] APE1 is a key enzyme in NER-based DNA repair.[44] We measured APE1 expression in the lens capsule before and after UVB irradiation. As shown in Figures 4E to 4H, a positive APE1 immunofluorescence stain was only seen in the germinative zone of the control lens capsule. However, after UVB irradiation, a significant amount of APE1 expression was observed at the perimeter, adjacent to the ring-shaped structure in the central lens capsule. Immunoblot analysis also confirmed that UVB induced APE1 expression (Fig. 4I). These results suggest that lens epithelial cells experience an ongoing, active repair process.

We checked the ultrastructure of the ring-shaped structure by TEM. As shown in Figures 3F and 3G, active phagocytosis was found in the front line of active repairing epithelial cells, such as cell A in Figures 3F and 3G, as they were "cleaning up" the residual cellular compartments of the damaged cells, such as cell B (narrow shape) and C (balloon shape) in Figures 3F and 3G, suggesting that the active proliferated lens epithelial cells were moving along the edge of the damaged zone to clean apoptotic cells. Aside from ultrastructural analysis, there are no specific markers to define the phagocytotic activity in various types of epithelial cells. However, mounting evidence suggests that epithelial cells possess dedicated receptors that can recognize the dying cells.[45] The $\alpha v\beta 5$ integrin is considered one of the key receptors that recognizes the classic "eat-me" signal from the apoptotic cells and has been found to be an essential molecule in phagocytosis of apoptotic cell debris by the lens epithelial cells.[46] For this reason, we measured $\beta 5$ integrin expression in the lens capsule of control and UVB-irradiated mice. As shown in Figures 4A to 4D, compared with the control lens capsule UVB irradiation increased $\beta 5$ integrin expression in the area outside the UVB-damaged zone, and it was significantly elevated at the perimeter, adjacent to the ring-shaped structure in the central capsule. We did not observe increased $\beta 5$ integrin expression in lens epithelial cells inside the UVB-damaged zone. Immunoblot analysis also confirmed that $\beta 5$ integrin expression was upregulated in UVB irradiated lens capsules compared to control capsules (Fig. 4I).

To further track the lens epithelial cell repair after UVB irradiation, we continued monitoring the lens capsular opacity using a slit lamp for up to 184 days after UVB irradi-

Investigative Ophthalmology & Visual Science

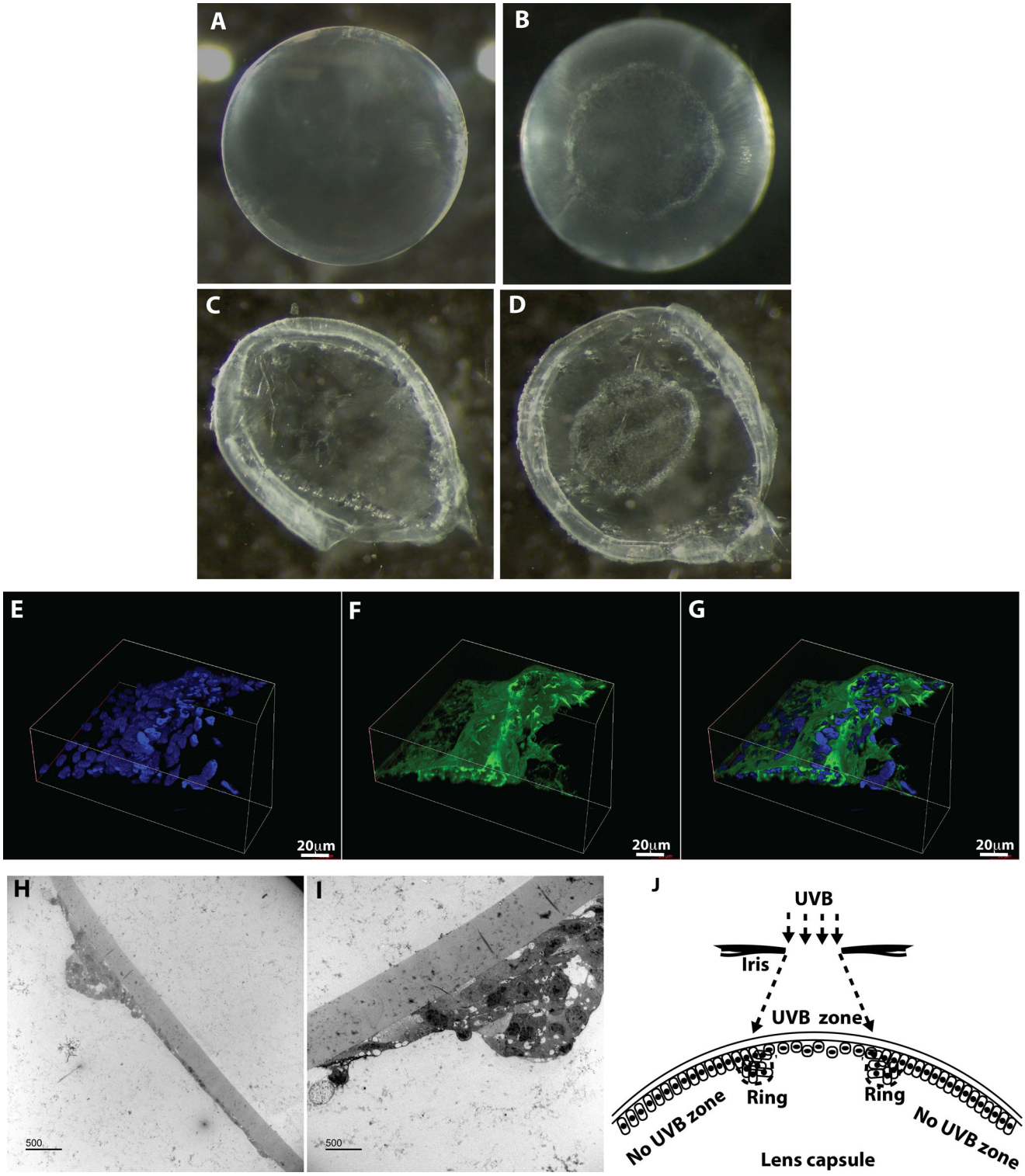

Figure 1. UVB induced lens epithelium damage and multi–cell-layer, ring-shaped dense opacity. Three-month-old mice ($n = 5$) were exposed to 24.7 kJ/m^2 of UVB, and capsular cataracts were documented at day 4 after irradiation. Darkfield images of (**A**) control lens, (**B**) UVB irradiated lens, (**C**) control lens capsule, and (**D**) UVB irradiated lens capsule. (**E–G**) The ring-shaped structure resulted from UVB irradiation that was immunofluorescently stained with F-actin. (**E**) Nuclei stained with Hoechst 33342. (**F**) Cellular cytoskeleton stained with F-actin antibody. (**G**) Merged image of **E** and **F**. (**H–J**) TEM of the lens capsule after UVB irradiation ($n = 2$). (**H**) Overview of the ring-shaped structure and adjacent epithelial monolayer. (**I**) Ultrastructure of the ring-shaped region. (**J**) Topographic view of the UVB-induced lens epithelium damage and ring-shaped opacity.

Investigative Ophthalmology & Visual Science

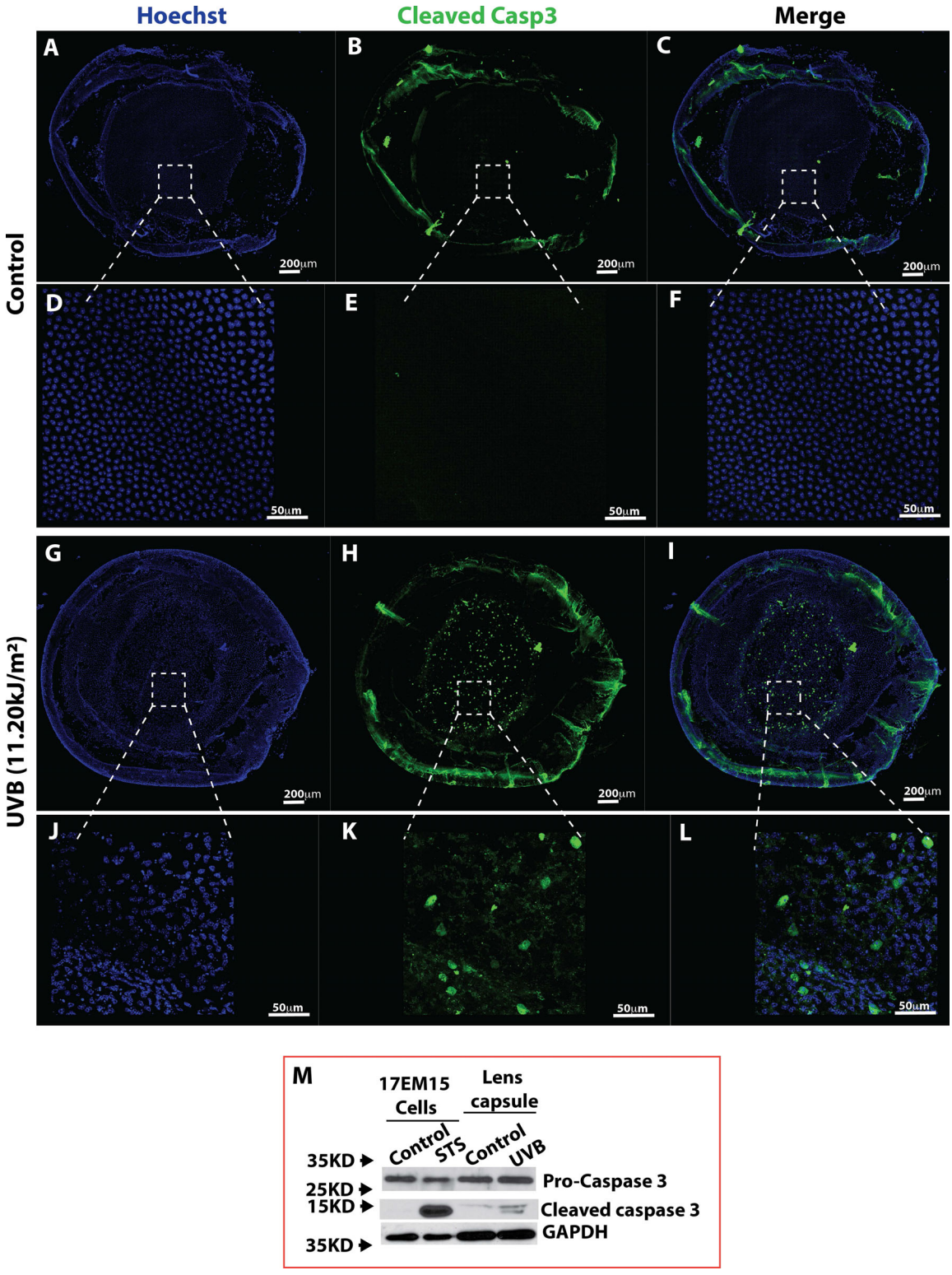

Figure 2. UVB induced lens epithelial cell apoptosis in the exposed zone. Three-month-old mice ($n = 5$) were exposed to 24.7 kJ/m^2 of UVB, and epithelium-cleaved caspase 3 was documented on day 4 after irradiation. (**A–F**) Control lens capsule stained by the cleaved caspase 3 antibody and Hoechst 33342. (**A**) Nuclei probed by Hoechst. (**B**) Cleaved caspase 3 immunofluorescence. (**C**) Merged image of **A** and **B**. (**D**) Magnified image from the selected region in **A**. (**E**) Magnified image from the selected region in **B**. (**F**) Magnified image from the selected region in **C**. (**G–L**) UVB-irradiated lens capsule stained by the cleaved caspase 3 antibody and Hoechst 33342. (**G**) Nuclei probed by Hoechst. (**H**) Cleaved caspase 3 immunofluorescence. (**I**) Merged image of **G** and **H**. (**J**) Magnified image from the selected region in **G**. (**K**) Magnified image from the selected region in **H**. (**L**) Magnified image from the selected region in **I**. (**M**) Immunoblot determination of pro- and cleaved caspase 3 in UVB-irradiated lens capsule compared with the unexposed lens capsule. Mouse lens epithelial cell line 17EM15 treated with or without 1-μM STS served as a positive control, and GAPDH was used as a loading control.

Investigative Ophthalmology & Visual Science

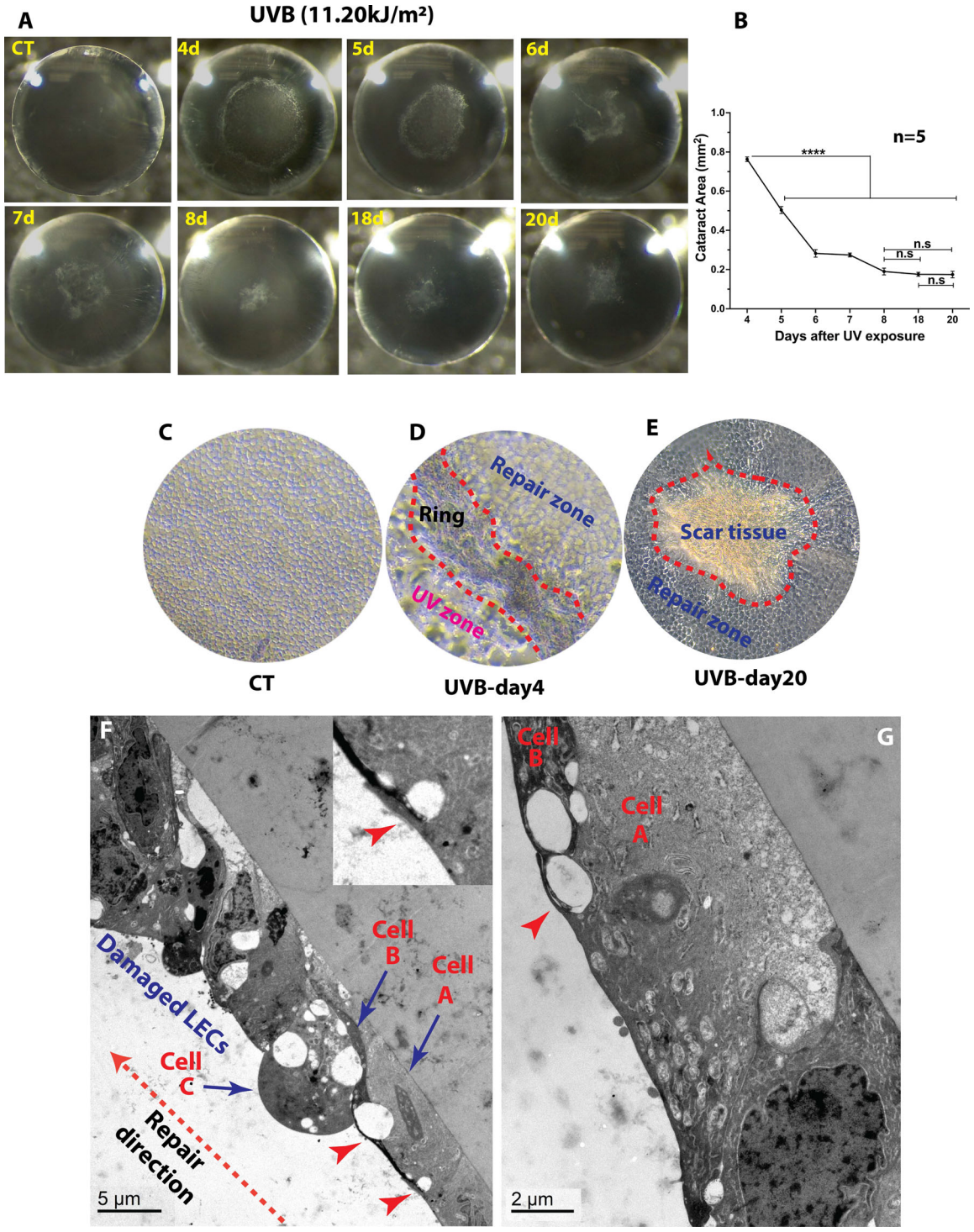

Figure 3. Lens epithelial cell repair via the epithelialization process. Three-month-old mice ($n = 5$) were exposed to 11.20 kJ/m^2 of UVB, and capsular cataracts were documented by darkfield and phase-contrast microscopy. The ultrastructure of frontline repair was analyzed by TEM after irradiation. The grade of the capsular cataract was calculated by measuring the area (mm^2) of the cataract. (**A**) Darkfield image of capsular cataracts and ring-shaped structure of mouse lenses unexposed and exposed to UVB from day 4 to day 20. (**B**) The area of capsular cataract was quantitatively determined with ImageJ. (**C**) A phase-contrast image of UVB-unexposed control lens capsule. (**D**) A phase-contrast image of a lens capsule near the ring-shaped region 4 days after UVB irradiation. A higher magnification relative to **C** was used. (**E**) A phase-contrast image of a lens capsule near the center of the anterior capsule showing scar-like tissue 20 days after UVB irradiation. (**F**) Ultrastructure of the lens capsule immediately outside of the ring-shaped structure obtained by TEM. The *red arrow* with a dotted line shows the path of lens epithelialization. *Blue arrows* point to individual cells. Cell A is the frontline healthy epithelial cell that is in the repair process. Cells B and C are damaged cells or residual cell compartments in the process of being removed by cell A via phagocytosis. *Red arrows* point to active phagocytosis from cell A. (**F**, inset) Higher magnification image of active phagocytosis from cell A. (G) Another representative ultrastructural image of active phagocytosis from the frontline repair epithelial cells. Cell A, healthy epithelial cell; cell B, damaged cell/cellular compartments. The *red arrow* points to active phagocytosis from cell A. Results are expressed as mean ± SD and were analyzed using one-way ANOVA with Tukey's multiple comparisons test. Only $P < 0.05$ was considered significant. *$P < 0.05$, **$P < 0.01$, ***$P < 0.001$, ****$P < 0.0001$; ns, not significant.

Investigative Ophthalmology & Visual Science

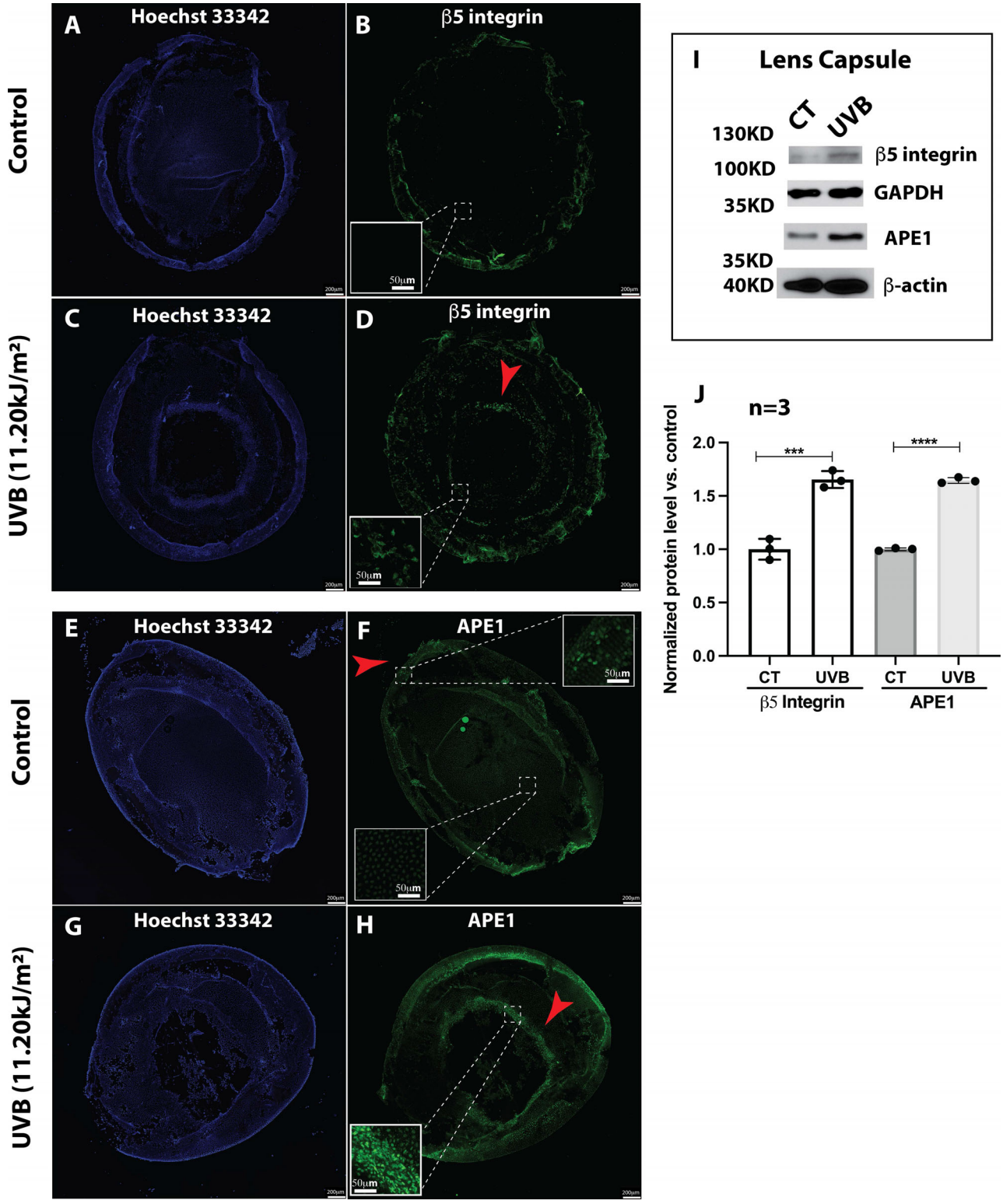

Figure 4. UVB irradiation induced $\beta 5$ integrin and DNA repair enzyme APE1 expression. Three-month-old mice ($n = 5$) were exposed to 11.20 kJ/m^2 of UVB. The $\beta 5$ integrin expression was measured by immunofluorescence stain using an anti-$\beta 5$ integrin antibody. (**A**, **B**) Unexposed control lens capsule. (**A**) Nuclei stained with Hoechst 33342. (**B**) The $\beta 5$ integrin stain. (**C**, **D**) Lens capsule 4 days after UVB irradiation. (**C**) Nuclei stained with Hoechst 33342. (**D**) The $\beta 5$ integrin stain is shown in *green*. The *red arrows* point to areas with positive $\beta 5$ integrin expression. The APE1 expression was measured by immunofluorescence stain using an anti-APE1 antibody. (**E**, **F**) unexposed control lens capsule. (**E**) Nuclei stained with Hoechst 33342. (**F**) APE1 stain. (**G**, **H**) Les capsule 4 days after UVB irradiation. (**G**) Nuclei stained with Hoechst 33342. (**H**) APE1 stain is shown in *green*. The *red arrows* point to areas with positive APE1 expression. (**I**) Immunoblot analysis of both $\beta 5$ integrin and APE1 protein levels in lens capsules from control and UVB-irradiated mice. GAPDH was used as a loading control for $\beta 5$ integrin, and β-actin was used as a loading control for APE1. (**J**) Semiquantitative results of $\beta 5$ integrin and APE1 based on immunoblot assay ($n = 3$). Insets are amplified images of selected regions. Results are expressed as mean ± SD and were analyzed using Student's *t*-test. Only $P < 0.05$ was considered significant. *$P < 0.05$, **$P < 0.01$, ***$P < 0.001$, ****$P < 0.0001$.

Investigative Ophthalmology & Visual Science

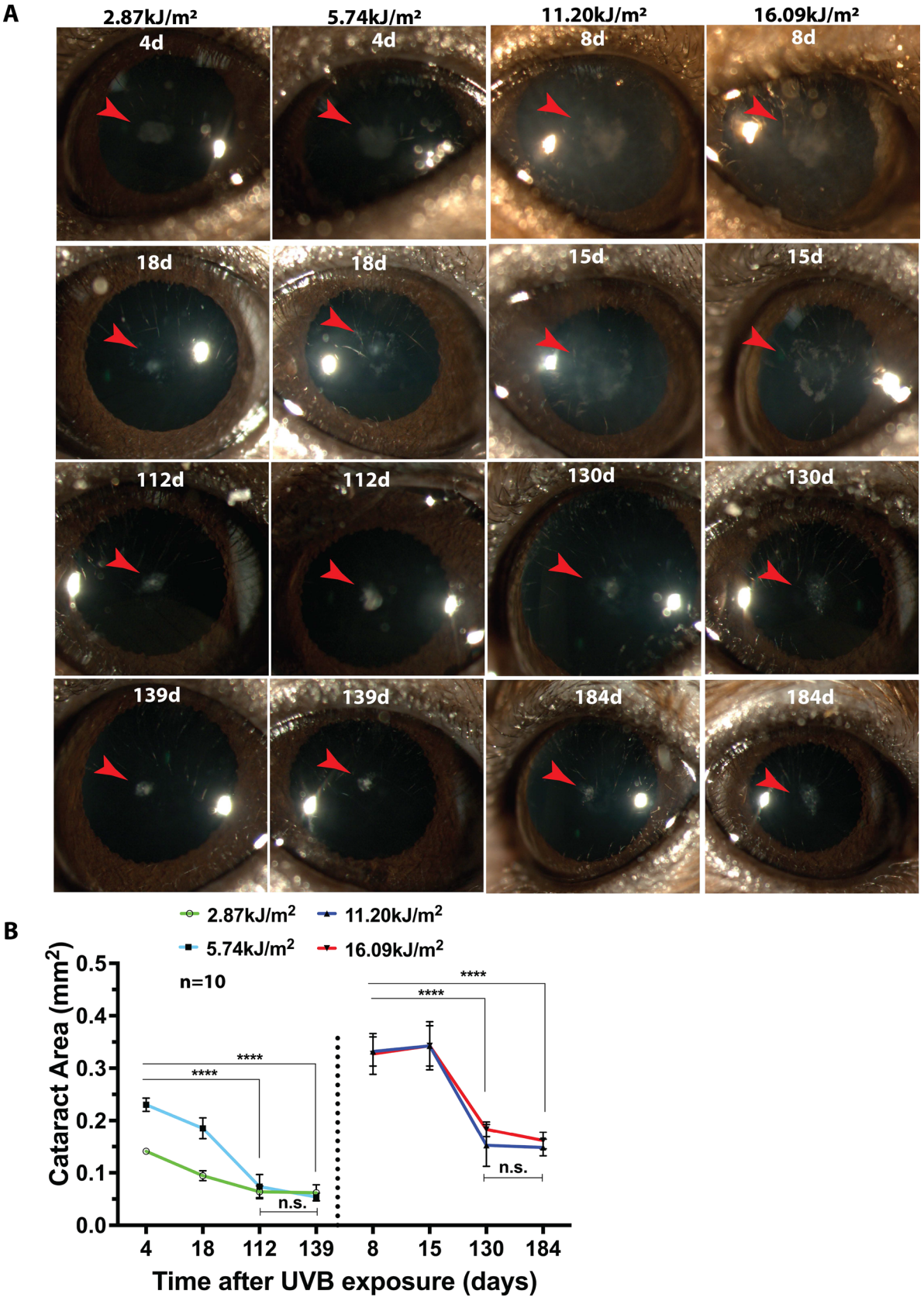

Figure 5. Time course of lens capsular cataract repair. Three-month-old mice ($n = 5$) were exposed to 2.87, 5.74, 11.20, and 16.09 kJ/m^2 of UVB. Capsular cataracts were monitored by a slit lamp periodically. The grade of the capsular cataract was calculated by measuring the area (mm^2) of the cataract. The *red arrows* point to capsular cataracts. (**A**) Slit-lamp images at various time points. (**B**) The area of capsular cataract quantitatively determined by ImageJ software ($n = 10$). Results are expressed as mean ± SD and were analyzed using one-way ANOVA with Tukey's multiple comparisons test. Only $P < 0.05$ was considered significant. *$P < 0.05$, **$P < 0.01$, ***$P < 0.001$, ****$P < 0.0001$; ns, not significant.

Investigative Ophthalmology & Visual Science

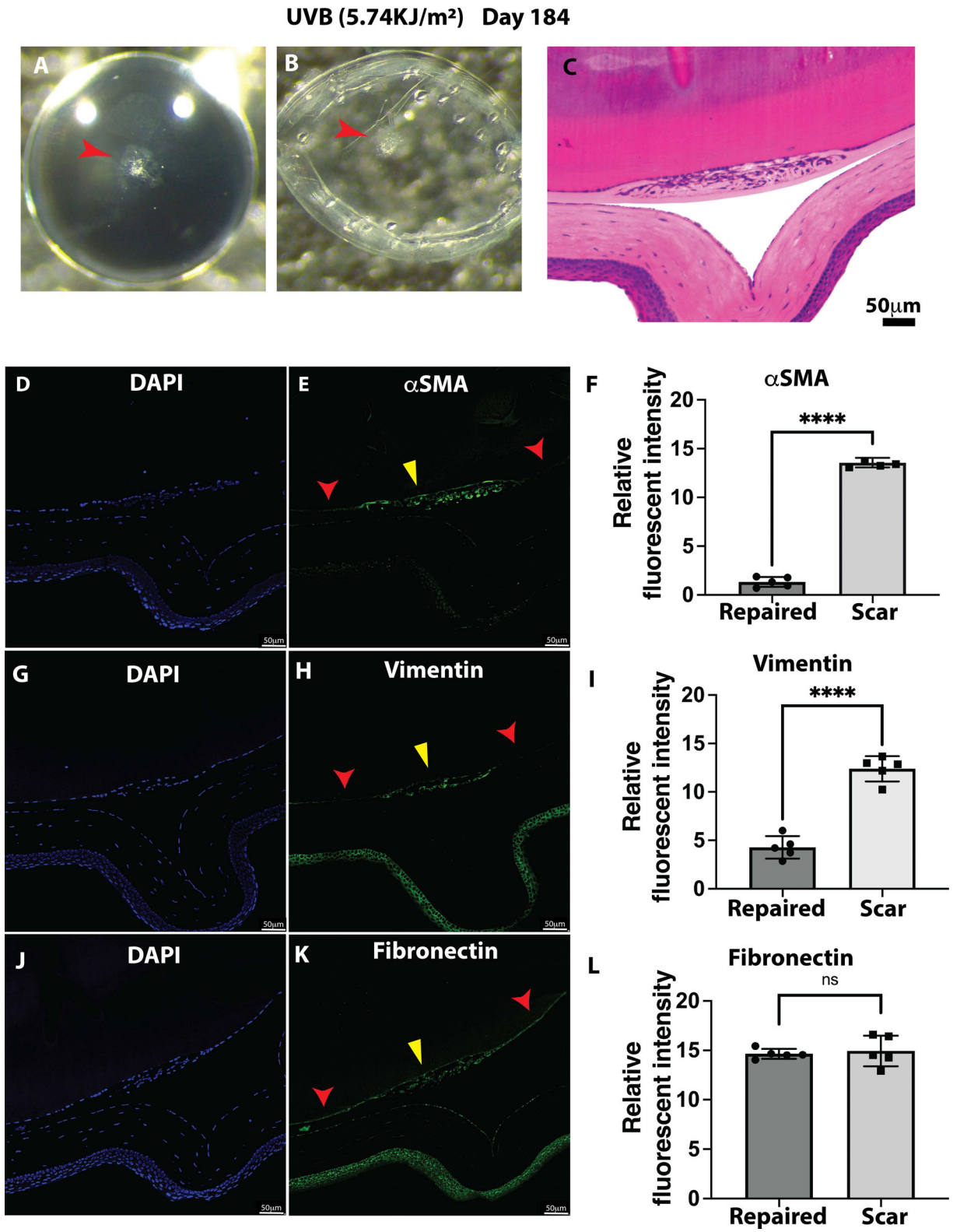

Figure 6. Incomplete repair and formation of scar-like tissue 6 months after UVB irradiation. Three-month-old mice ($n = 5$) were exposed to 5.74 kJ/m^2 of UVB. Capsular cataracts at day 184 after UVB irradiation were measured by lens and capsule phase-contrast imaging and H&E histology. (**A**) Lens image. (**B**) Lens capsule image. (**C**) H&E histological image. (**D–L**) Fibrosis markers, αSMA, vimentin, and fibronectin, were determined by immunofluorescence stain using the proper antibodies. *Red arrows* point to fully repaired lens epithelium, and *yellow arrows* point to the scar tissue. Both αSMA and vimentin were highly expressed in the scar-like tissue. (**D**) Nuclei stained with DAPI. (**E**) αSMA is shown in *green*. (**F**) Statistical comparison of αSMA relative fluorescent intensity between repaired epithelium and scar tissue. (**G**) Nuclei stained with DAPI. (**H**) Vimentin is shown in *green*. (**I**) Statistical comparison of vimentin relative fluorescent intensity between repaired epithelium and scar tissue. (**J**) Nuclei stained with DAPI. (**K**) Fibronectin is shown in *green*. (**L**) Statistical comparison of fibronectin relative fluorescent intensity between repaired epithelium and scar tissue. Results are expressed as mean ± SD and were analyzed using Student's *t*-test. Only $P < 0.05$ was considered significant. *$P < 0.05$, **$P < 0.01$, ***$P < 0.001$, ****$P < 0.0001$.

ation. Representative images selected from four time points are illustrated in Figure 5A. Additional slit-lamp images of five experimental mice at selected time points are provided in Supplementary Figures S2 to S5. The quantitative sizes of the capsular cataracts are summarized in Figure 5B. Large sizes of capsular opacity were seen at day 4 after the 2.87-kJ/m^2 and 5.74-kJ/m^2 doses and at day 8 after the 11.20-kJ/m^2 and 16.09-kJ/m^2 UVB irradiation. Interestingly, the cornea was directly impacted by UVB irradiation, and an initial loss of transparency was observed in mice 24 to 72 hours and 1 to 8 days after 2.87-kJ/m^2 and 5.74-kJ/m^2 UVB irradiation and after 11.20-kJ/m^2 and 16.09-kJ/m^2 UVB irradiation, respectively. However, the corneal repair seemed to be much faster and more complete than the lens repair. Eight days after UVB irradiation, a transparent cornea was seen and the transparency was maintained throughout the end of the study (>130days). Intrudingly, in all tested UVB doses, the lens epithelium stopped its repair activity when the opacity reached the anterior capsule center. We did not see remarkable changes in the size of capsular opacity from 112 to 139 days in the 2.87-kJ/m^2 and 5.74-kJ/m^2 irradiated mice and from 130 days to 184 days in the 11.20-kJ/m^2 and 16.09-kJ/m^2 UVB irradiated mice.

To check the partially repaired opacity structure, we dissected mice lenses at 184 days after 5.74-kJ/m^2 UVB irradiation. Figure 6A shows the lens darkfield image, and the capsular opacity can clearly be seen at the center of the anterior capsule. The opacification was also observed when we dissected the lens capsule (Fig. 6B). The histology section with hematoxylin and eosin (H&E) stain (Fig. 6C) indicated that clusters of irregularly stacked cells formed the capsular opacity. The morphology (Fig. 3E) of the remaining unrepaired capsular cataracts seems to be a scar-like tissue. To confirm this, we performed an immunofluorescence staining with three fibrosis markers, αSMA, vimentin, and fibronectin. As shown in Figures 6D to 6I, compared with repaired lens capsules the unrepaired tissue showed ~eightfold and ~threefold increases in αSMA and vimentin expression, respectively, a strong indication of scar-like tissue types. We did not see significant changes in fibronectin expression between repaired and unrepaired tissues (Figs. 6J–6L).

Mitotic Activation of the Lens Epithelial Cells Around Wound Edges Is Responsible for Capsular Cataract Repair

The rapid epithelialization after UVB irradiation by lens epithelial cells inspired us to study its potential mechanisms. First, we observed that the dense, ring-shaped structure was formed around 4 days after UVB irradiation. Second, we saw rapid shrinking of the ring size with time. Finally, we noticed that the ring-shaped structure disappeared when central, scar-like tissue was formed. We tested the active cell proliferation zone by staining the lens capsule with an antibody specific for Ki67, a cell proliferation marker. As shown in Figures 7A to 7C, the control lens capsule without UVB irradiation only showed a positive Ki67 stain at the germinative zone (lens equator). Of note, the positive Ki67 stain demonstrated a punctate pattern colocalized with cell nuclei (stained by Hoechst 33342). The dispersed green background was due to a non-specific stain. Again, at the edge of the capsule, tissue folding after dissection also gave rise to some non-specific signals. Interestingly, 4 days after UVB irradiation, the most active cell proliferation was at the edge of the ring-shaped structure (Figs. 7D–7F). These results indicate that the once quiescent epithelial cells reactivate their cell cycle and convert to highly proliferative epithelial cells for repair purposes.

Lens Epithelial Cells Cease the Epithelialization Process When Epithelial Cells Are in Direct Contact

The lens epithelial cells around the edge of the wound initialized a rapid epithelialization process, but repair stopped soon after the damaged epithelial cells accumulated in the center of the anterior capsule. We checked the status of mitotically activated epithelial cells through Ki67 antibody staining, and no Ki67-positive epithelial cells were seen around the scar-like tissue 186 days after UVB irradiation (Figs. 7G–7I). From the H&E histology (Fig. 6C), we noticed that the epithelial monolayer crossing the damaged zone had already formed, and the opacity was due to the damaged, but not absorbed, epithelial cells being stacked between the epithelial monolayer and the lens capsule. These results suggest that, when the active repairing lens epithelial cells make direct contact, the proliferation ceases, and epithelialization ends, likely by the mechanism of cell–cell contact inhibition.

To further confirm our findings, we labeled active proliferating lens epithelial cells by BrdU incorporation. As shown in Figures 8A and 8B, BrdU was seen only at the germinative zone of the lens capsule in control mice without UVB irradiation. In contrast, 4 days after UVB irradiation, massive BrdU labeling was seen around the edge of the ring-shaped structure. Consistent with Ki67 staining, no BrdU-positive stain was observed around the edge of the scar-like tissue in the capsule 186 days after UVB irradiation. Instead, BrdU was seen only at the germinative zone of the lens capsule.

Discussion

In the present study, we studied the wound healing response of lens epithelial cells using the UVB irradiation mouse model, a well-established mouse cataract model.[33,35] UVB irradiation above a dose of 2.87 kJ/m^2 triggered lens epithelial cell apoptosis and subcapsular cataract formation. A ring-shaped structure composed of multilayered epithelial cell clusters manifested as a dense ring-shaped capsular cataract. The epithelial cells immediately outside the edge of these ring-shaped aggregates transitioned into mitotically active cells and performed wound healing with an epithelialization process. Although it was not completely repaired, the damaged area shrunk significantly, with only a small scar-like tissue remaining in the center of the anterior capsule 6 months after UVB irradiation. This study and these observations originated from our attempt to establish a UVB-induced mouse cataract model. Some of our findings, such as the subcapsular cataract formation and repair phenomena, echoed the findings of studies by others.[33,35] For example, Meyer et al.[47] found that the maximum tolerable dose at which C57BL/6J mice developed cataracts was 2.9 kJ/m^2, a dosage essentially equal to our finding (2.87 kJ/m^2). Similarly, the rapid epithelium repair within 8 days of UVB irradiation was also reported by Zhang et al.[35] in their UVB-induced mouse model study. However, the scale of epithelial cell apoptosis was different compared with the previous report. In the threshold-dose UVB-induced rat

Investigative Ophthalmology & Visual Science

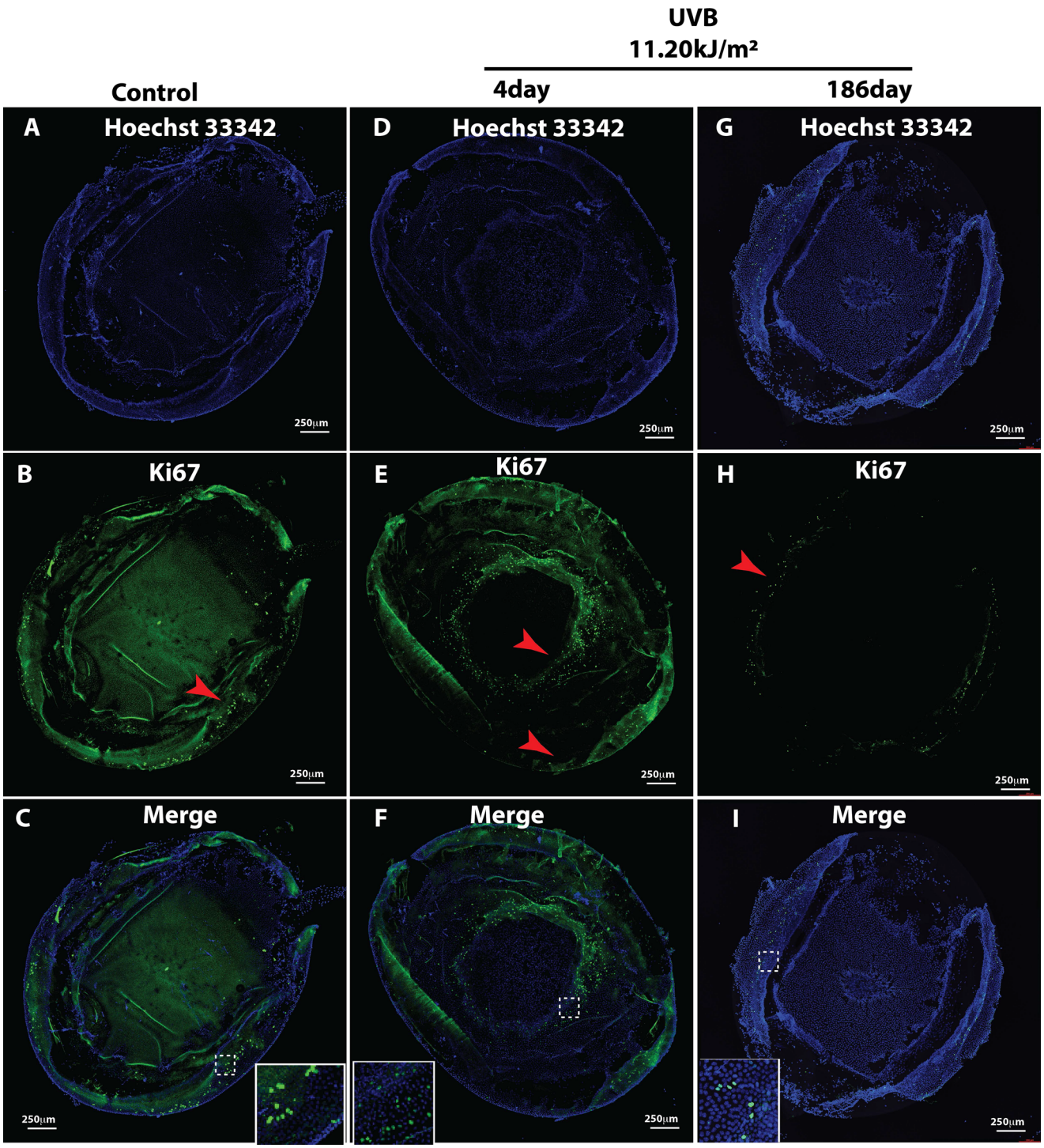

Figure 7. Cell-cycle reactivation of lens epithelial cells at the edge of UVB-damaged epithelium. Three-month-old mice (n = 5) were exposed to 11.20 kJ/m^2 of UVB. Unexposed control and UVB-exposed mouse lens capsules were immunofluorescently stained with Ki67. (**A–C**) unexposed control lens capsule. (**A**) Nuclei stained with Hoechst 33342. (**B**) Ki67 stain. (**C**) Merged image of **A** and **B**. (**D–F**) Lens capsules 4 days after UVB irradiation. (**D**) Nuclei stained with Hoechst 33342. (**E**) Ki67 stain. (**F**) Merged image of **D** and **E**. (**G–I**) Lens capsules 184 days after UVB irradiation. (**G**) Nuclei stained with Hoechst 33342. (**H**) Ki67 stain. (**I**) Merged image of **G** and **H**. (**C**, **F**, **I**, insets) Higher magnification image of the selected region is indicated by the *white dotted square*.

cataract study, apoptosis was detected in the entire lens epithelium.[38] However, we only observed apoptotic epithelial cells in the UVB-exposed zone and did not detect apoptotic cells in the germinative zone. Whether this discrepancy is related to different species requires further clarified.

Lens epithelium is located at the anterior of the lens. It is composed of a monolayer of lens epithelial cells that

Investigative Ophthalmology & Visual Science

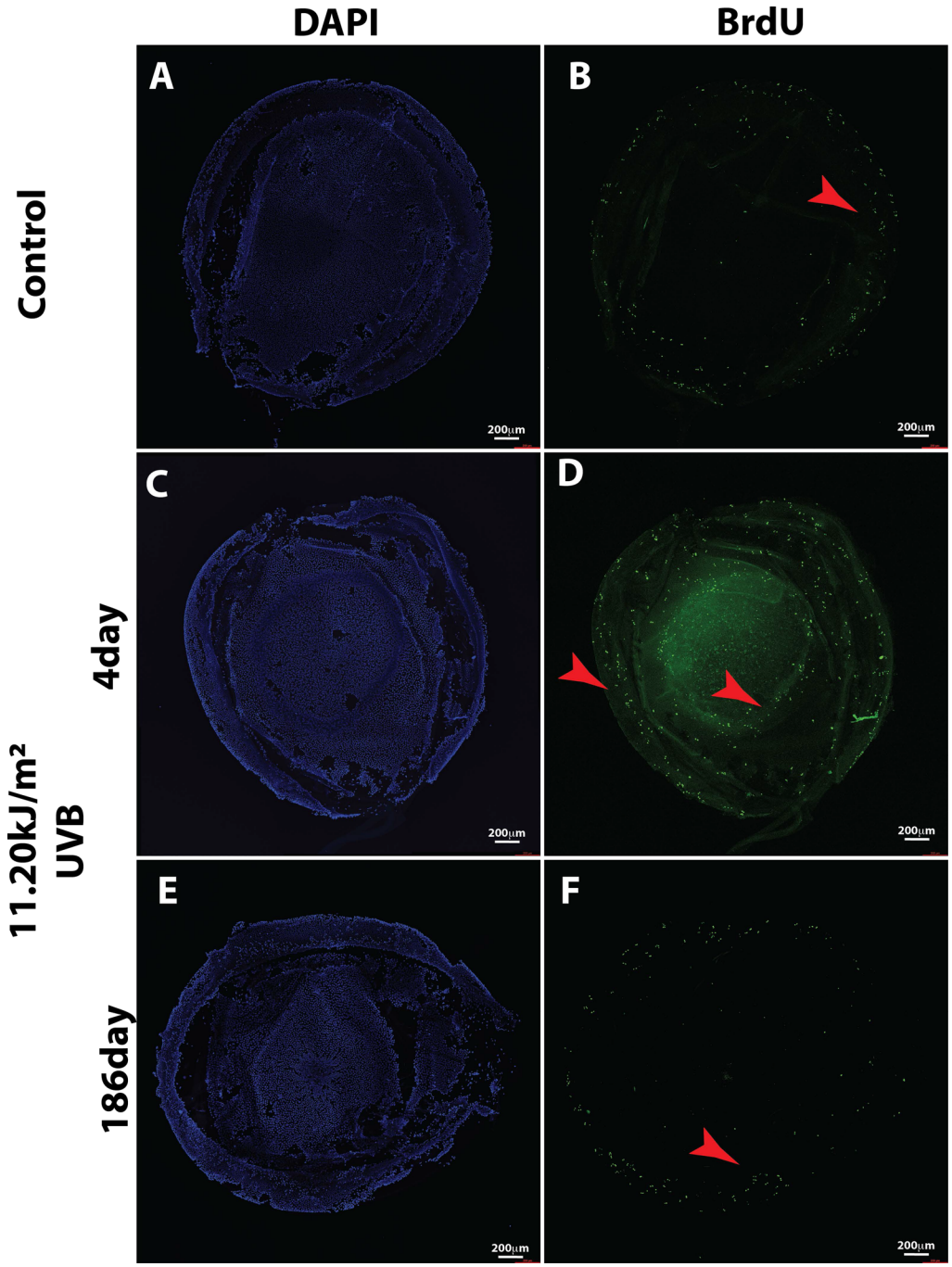

Figure 8. Active S-phase of the cell cycle of lens epithelial cells at the edge of UVB-damaged epithelium probed by BrdU incorporation. Three-month-old mice ($n = 5$) were exposed to 11.20 kJ/m^2 of UVB. The S-phase cell cycle was tracked by BrdU incorporation. (**A**, **B**) Unexposed control lens capsule. (**A**) Nuclei stained with Hoechst 33342. (**B**) BrdU is indicated by the *green punctate pattern*. The *red arrow* points to an area with positive BrdU incorporation. (**C**, **D**) Lens capsule 4 days after UVB irradiation. (**C**) Nuclei stained with Hoechst 33342. (**D**) BrdU is indicated by the *green punctate pattern*. The *red arrows* point to areas with positive BrdU incorporation. (**E**, **F**) Lens capsules 184 days after UVB irradiation. (**E**) Nuclei stained with Hoechst 33342. (**F**) BrdU is indicated by the *green punctate pattern*. The *red arrow* points to an area with positive BrdU incorporation.

continuously proliferate throughout their lifetime, and these cells are the only ones in the lens that can proliferate.[48,49] Not all lens epithelial cells are equal in terms of cell proliferation, as the lens epithelium is divided into several distinct regions. For example, McAvoy[49] classified the lens epithelium into three zones: anterior, germinative, and transition. Sikic et al.[50] further classified the lens epithelium into four zones: central, pre-germinative, germinative, and transition. Lens epithelial cells in the germinative zone, also known as the lens equator, are mitotically active. Epithelial cells in the pre-germinative region are also mitotically active but to a lesser degree than epithelial cells in the germinative zone, and the epithelial cells in the transition zone are in the process of cell differentiation into fiber cells. In comparison,

Investigative Ophthalmology & Visual Science

the epithelial cells in the central/anterior zone are considered quiescent cells—in other words, mitotically inactive cells. Using Ki67 immunostaining to detect mitotic active cells and BrdU incorporation to probe active cell S-phase DNA synthesis, we also confirmed that only epithelial cells in the germinative zone are mitotically active in normal lens epithelium. The mitotically active epithelial cells that are only found in the germinative region would explain the prediction by Meyer et al.[39] In their TEM-based ultrastructural study of the mouse lens epithelium repair phenomena mediated by UVB irradiation, they predicted that a full repair through epithelial cells would originate from the division of those epithelial cells located in the germinative zone.[39] However, in this study, we discovered that, after UVB irradiation, epithelial cells in the central zone positioned immediately next to damaged cells underwent cell cycle reactivation, and the cells became mitotically active. These actively proliferating epithelial cells migrate along the lens capsule via epithelialization to remove and repair the damaged and apoptotic cells. Our study indicated that the quiescent lens epithelial cells in the central region could be reactivated once adjacent epithelial cells were damaged. Interestingly, we found that the epithelization process would be terminated when the epithelial cells came in direct contact and a monolayer formed. The molecular nature of lens cell cycle reactivation and contact inhibition should be elucidated in future studies. The scar tissue resulting from contact inhibition demonstrates a highly fibrotic phenotype with markedly elevated αSMA and vimentin levels. Studies have shown that lens epithelial cells can produce a significant amount of these fibrotic molecules during transdifferentiation, often through epithelial–mesenchymal transition (EMT).[51,52] More studies are necessary to understand the potential involvement of the EMT process in scar tissue formation after UVB irradiation. Interestingly, Menko et al.[53] found that vimentin-rich lens epithelial cells at the leading edge regulated cell movement during wound healing. This may explain the high vimentin content in the scar tissue induced by UVB irradiation. The remaining unrepaired tissue originates from the ring-shaped structure closure, a cluster of leading-edge migrating lens epithelial cells.

Phagocytosis is a highly complex process of ingesting and eliminating pathogens, apoptotic cells, and cellular debris.[54] Cells with high phagocytotic efficiency, such as macrophages, neutrophils, and monocytes, are referred to as professional phagocytes.[55] However, it is well known that epithelial cells, endothelial cells, and fibroblasts can also engulf cell debris and particles, and these are often considered the non-professional phagocytes.[45] Early study has demonstrated that the phagocytotic process of lens epithelial cells plays an essential role in lens development by cleaning up apoptotic cells.[56] Lens epithelial cells have also been found to be capable of repairing an injury through phagocytosis,[57,58] and they attempt to remove cell debris in the early stage of cortical cataract development.[59] Using both a human lens epithelial cell line and chicken primary epithelial cells, Chauss et al.[46] showed that lens epithelial cells were able to take up and ingest apoptotic cell debris and bacterial particles. Importantly, they determined that αVβ5 integrin is required for lens epithelial cells to recognize apoptotic cell debris for subsequent ingestion.

Our findings also indicate that the frontline, actively repairing lens epithelial cells remove the damaged epithelial cells and residual cellular compartments through phagocytosis, as we observed active phagocytosis in the TEM study. Interestingly, we found significantly elevated β5 integrin expression at the perimeter of the ring-shaped structure. This likely indicates increased αVβ5 levels at the ring-shaped region, as the β5 subunit has been found to form heterodimers with the αV subunit.[60] The study also showed that elevated intracellular β5 integrin expression could significantly increase αVβ5 integrin activity.[61] Phosphatidylserine is a phospholipid that can be exposed to the external leaflet of apoptotic cells and can be recognized by the receptors of phagocytes. The αVβ5 integrin has been widely studied as a cell surface receptor that recognizes and binds phosphatidylserine. In addition to lens epithelial cells,[46] αVβ5 integrin has also been found to be an essential receptor used by the retinal pigment epithelium (RPE) to remove the degradation debris from the photoreceptor outer segment via phagocytosis.[62] After UVB irradiation, the availability of αVβ5 integrin at the lens epithelial cell surface signifies that it will be readily available to recognize apoptotic cells and their debris through phagocytosis. Furthermore, our TEM results are in agreement with the *in vitro* studies of UVB-irradiated human lens epithelial cells, indicating that the UVB-damaged cellular compartment was phagocytosed by neighboring living cells.[63] Similarly, phagosomes have also been observed in the mouse epithelium after UVB irradiation.[39,57] We believe that a rapid epithelization process and relatively slow endocytosis and repair processes push damaged epithelial cells into an irregular, multi–cell layer, ring-shaped structure. However, there are no specific biomarkers available to allow explicit determination of the status of phagocytosis in non-professional phagocytes. The increased β5 integrin expression is a piece of indirect evidence suggesting the existence of elevated phagocytotic activity in actively repairing lens epithelial cells. Additionally, β5 integrin binds ligands containing an RGD motif, such as vitronectin,[64] which is present in the lens epithelial cells of the intact lens.[65] Further studies are necessary to better understand the relationship between increased αVβ5 integrin expression and phagocytosis activity.

In summary, our present study has demonstrated that quiescent lens epithelial cells can be reprogrammed for proliferation to repair the damaged lens epithelium. Normal lens epithelial cells are essential in lens development and postnatal lens growth, although, under stress or cell damage, they may present unique features of cellular repair. Studies have demonstrated that lens epithelial cells possess an endogenous stem cell-like function.[66] Their proliferation/self-renewal is a critical component in the lens regeneration process, and it has attracted considerable attention in recent years.[67–69] Our study provides strong evidence that lens epithelial cells maintain a significant proliferation potential in response to UV. These stem cell–like characteristics of lens epithelial cells might be the biological foundation for the self-repair mechanism in the lens. We also want to emphasize that UVB-induced damage and repair in the lens may serve as an ideal model for a broad range of researchers who are interested in regenerative medicine.

Acknowledgments

The authors are very grateful to Salil Lachke, PhD, at the University of Delaware for providing the mouse lens epithelial cell line and to Rachel Cui, PhD, at the Augusta University Cell Imaging Core for helping with the microscopy image collections. We are also grateful to Brendan Marshall, PhD, at the Augusta

University Electron Microscopy/Histology Core Laboratory for helping in the electron microscopy study.

Supported by grants from the National Eye Institute, National Institutes of Health (EY028158 to XF), by a National Eye Institute Center Core Grant for Vision Research (P30EY031631) at Augusta University, by a grant from the BrightFocus Foundation (M2015180 to HLW), and by a California Table Grape Commission Research Grant (HLW).

Disclosure: **Z. Wei**, None; **C. Hao**, None; **R. Srinivasagan**, None; **H. Wu**, None; **J.-K. Chen**, None; **X. Fan**, None

References

1. Rafnsson V, Olafsdottir E, Hrafnkelsson J, Sasaki H, Arnarsson A, Jonasson F. Cosmic radiation increases the risk of nuclear cataract in airline pilots: a population-based case-control study. *Arch Ophthalmol*. 2005;123:1102–1105.
2. Cadet JM, Bencherif H, Cadet N, et al. Solar UV radiation in the tropics: human exposure at Reunion Island (21 degrees S, 55 degrees E) during summer outdoor activities. *Int J Environ Res Public Health*. 2020;17:8105.
3. Sasaki K, Sasaki H, Kojima M, et al. Epidemiological studies on UV-related cataract in climatically different countries. *J Epidemiol*. 1999;9:S33–S38.
4. Roberts JE. Ultraviolet radiation as a risk factor for cataract and macular degeneration. *Eye Contact Lens*. 2011;37:246–249.
5. Ivanov IV, Mappes T, Schaupp P, Lappe C, Wahl S. Ultraviolet radiation oxidative stress affects eye health. *J Biophotonics*. 2018;11:e201700377.
6. Cruickshanks KJ, Klein BE, Klein R. Ultraviolet light exposure and lens opacities: the Beaver Dam Eye Study. *Am J Public Health*. 1992;82:1658–1662.
7. Taylor HR, West SK, Rosenthal FS, et al. Effect of ultraviolet radiation on cataract formation. *N Engl J Med*. 1988;319:1429–1433.
8. Hollows F, Moran D. Cataract–the ultraviolet risk factor. *Lancet*. 1981;2:1249–1250.
9. Miyashita H, Hatsusaka N, Shibuya E, et al. Association between ultraviolet radiation exposure dose and cataract in Han people living in China and Taiwan: a cross-sectional study. *PLoS One*. 2019;14:e0215338.
10. Yu JM, Yang DQ, Wang H, et al. Prevalence and risk factors of lens opacities in rural populations living at two different altitudes in China. *Int J Ophthalmol*. 2016;9:610–616.
11. Kleiman NJ, Wang RR, Spector A. Ultraviolet light induced DNA damage and repair in bovine lens epithelial cells. *Curr Eye Res*. 1990;9:1185–1193.
12. Andley UP, Lewis RM, Reddan JR, Kochevar IE. Action spectrum for cytotoxicity in the UVA- and UVB-wavelength region in cultured lens epithelial cells. *Invest Ophthalmol Vis Sci*. 1994;35:367–373.
13. Andley UP, Hebert JS, Morrison AR, Reddan JR, Pentland AP. Modulation of lens epithelial cell proliferation by enhanced prostaglandin synthesis after UVB exposure. *Invest Ophthalmol Vis Sci*. 1994;35:374–381.
14. Mesa R, Bassnett S. UV-B-induced DNA damage and repair in the mouse lens. *Invest Ophthalmol Vis Sci*. 2013;54:6789–6797.
15. Osnes-Ringen O, Azqueta AO, Moe MC, et al. DNA damage in lens epithelium of cataract patients in vivo and ex vivo. *Acta Ophthalmol*. 2013;91:652–656.
16. Hott JL, Borkman RF. Concentration dependence of transmission losses in UV-laser irradiated bovine alpha-, beta H-, beta L- and gamma-crystallin solutions. *Photochem Photobiol*. 1993;57:312–317.
17. Mafia K, Gupta R, Kirk M, Wilson L, Srivastava OP, Barnes S. UV-A-induced structural and functional changes in human lens deamidated alphaB-crystallin. *Mol Vis*. 2008;14:234–248.
18. Weinreb O, van Boekel MA, Dovrat A, Bloemendal H. Effect of UV-A light on the chaperone-like properties of young and old lens alpha-crystallin. *Invest Ophthalmol Vis Sci*. 2000;41:191–198.
19. Reddy GB, Bhat KS. UVB irradiation alters the activities and kinetic properties of the enzymes of energy metabolism in rat lens during aging. *J Photochem Photobiol B*. 1998;42:40–46.
20. Tsentalovich YP, Sherin PS, Kopylova LV, Cherepanov IV, Grilj J, Vauthey E. Photochemical properties of UV filter molecules of the human eye. *Invest Ophthalmol Vis Sci*. 2011;52:7687–7696.
21. Bova LM, Sweeney MH, Jamie JF, Truscott RJ. Major changes in human ocular UV protection with age. *Invest Ophthalmol Vis Sci*. 2001;42:200–205.
22. Parker NR, Jamie JF, Davies MJ, Truscott RJ. Protein-bound kynurenine is a photosensitizer of oxidative damage. *Free Radic Biol Med*. 2004;37:1479–1489.
23. Linetsky M, Ortwerth BJ. Quantitation of the reactive oxygen species generated by the UVA irradiation of ascorbic acid-glycated lens proteins. *Photochem Photobiol*. 1996;63:649–655.
24. Ortwerth BJ, Prabhakaram M, Nagaraj RH, Linetsky M. The relative UV sensitizer activity of purified advanced glycation endproducts. *Photochem Photobiol*. 1997;65:666–672.
25. Linetsky M, Raghavan CT, Johar K, et al. UVA light-excited kynurenines oxidize ascorbate and modify lens proteins through the formation of advanced glycation end products: implications for human lens aging and cataract formation. *J Biol Chem*. 2014;289:17111–17123.
26. Fan X, Sell DR, Hao C, et al. Vitamin C is a source of oxoaldehyde and glycative stress in age-related cataract and neurodegenerative diseases. *Aging Cell*. 2020;19:e13176.
27. Fan X, Liu X, Hao S, Wang B, Robinson ML, Monnier VM. The LEGSKO mouse: a mouse model of age-related nuclear cataract based on genetic suppression of lens glutathione synthesis. *PLoS One*. 2012;7:e50832.
28. Blondin J, Baragi V, Schwartz E, Sadowski JA, Taylor A. Delay of UV-induced eye lens protein damage in guinea pigs by dietary ascorbate. *J Free Radic Biol Med*. 1986;2:275–281.
29. Andley UP, Patel HC, Xi JH, Bai F. Identification of genes responsive to UV-A radiation in human lens epithelial cells using complementary DNA microarrays. *Photochem Photobiol*. 2004;80:61–71.
30. Nakamura Y, Fukiage C, Azuma M, Shearer TR. Calpain-induced light scattering in young rat lenses is enhanced by UV-B. *J Ocul Pharmacol Ther*. 2001;17:47–58.
31. Azzam N, Levanon D, Dovrat A. Effects of UV-A irradiation on lens morphology and optics. *Exp Gerontol*. 2004;39:139–146.
32. Risa O, Saether O, Lofgren S, Soderberg PG, Krane J, Midelfart A. Metabolic changes in rat lens after in vivo exposure to ultraviolet irradiation: measurements by high resolution MAS 1H NMR spectroscopy. *Invest Ophthalmol Vis Sci*. 2004;45:1916–1921.
33. Meyer LM, Soderberg P, Dong X, Wegener A. UVR-B induced cataract development in C57 mice. *Exp Eye Res*. 2005;81:389–394.
34. Dong X, Ayala M, Lofgren S, Soderberg PG. Ultraviolet radiation-induced cataract: age and maximum acceptable dose. *Invest Ophthalmol Vis Sci*. 2003;44:1150–1154.
35. Zhang J, Yan H, Lofgren S, Tian X, Lou MF. Ultraviolet radiation-induced cataract in mice: the effect of age and

the potential biochemical mechanism. *Invest Ophthalmol Vis Sci*. 2012;53:7276–7285.
36. Huangfu J, Hao C, Wei Z, Wormstone IM, Yan H, Fan X. Cellular FLICE-like inhibitory protein (cFLIP) critically maintains apoptotic resistance in human lens epithelial cells. *Cell Death Dis*. 2021;12:386.
37. Wei Z, Caty J, Whitson J, et al. Reduced glutathione level promotes epithelial-mesenchymal transition in lens epithelial cells via a Wnt/β-catenin-mediated pathway: relevance for cataract therapy. *Am J Pathol*. 2017;187:2399–2412.
38. Michael R, Vrensen GF, van Marle J, Gan L, Soderberg PG. Apoptosis in the rat lens after in vivo threshold dose ultraviolet irradiation. *Invest Ophthalmol Vis Sci*. 1998;39:2681–2687.
39. Meyer LM, Wegener AR, Holz FG, Kronschlager M, Bergmanson JP, Soderberg PG. Ultrastructure of UVR-B-induced cataract and repair visualized with electron microscopy. *Acta Ophthalmol*. 2014;92:635–643.
40. Osakabe A, Tachiwana H, Kagawa W, et al. Structural basis of pyrimidine-pyrimidone (6-4) photoproduct recognition by UV-DDB in the nucleosome. *Sci Rep*. 2015;5:16330.
41. Sinha RP, Hader DP. UV-induced DNA damage and repair: a review. *Photochem Photobiol Sci*. 2002;1:225–236.
42. Maeda T, Chua PP, Chong MT, Sim AB, Nikaido O, Tron VA. Nucleotide excision repair genes are upregulated by low-dose artificial ultraviolet B: evidence of a photoprotective SOS response? *J Invest Dermatol*. 2001;117:1490–1497.
43. Budden T, Bowden NA. The role of altered nucleotide excision repair and UVB-induced DNA damage in melanomagenesis. *Int J Mol Sci*. 2013;14:1132–1151.
44. Thakur S, Sarkar B, Cholia RP, Gautam N, Dhiman M, Mantha AK. APE1/Ref-1 as an emerging therapeutic target for various human diseases: phytochemical modulation of its functions. *Exp Mol Med*. 2014;46:e106.
45. Gunther J, Seyfert HM. The first line of defence: insights into mechanisms and relevance of phagocytosis in epithelial cells. *Semin Immunopathol*. 2018;40:555–565.
46. Chauss D, Brennan LA, Bakina O, Kantorow M. Integrin αVβ5-mediated removal of apoptotic cell debris by the eye lens and its inhibition by UV light exposure. *J Biol Chem*. 2015;290:30253–30266.
47. Meyer LM, Dong X, Wegener A, Soderberg P. Dose dependent cataractogenesis and maximum tolerable dose (MTD(2.3:16)) for UVR 300 nm-induced cataract in C57BL/6J mice. *Exp Eye Res*. 2008;86:282–289.
48. Zwaan J, Kenyon RE, Jr. Cell replication and terminal differentiation in the embryonic chicken lens: normal and forced initiation of lens fibre formation. *J Embryol Exp Morphol*. 1984;84:331–349.
49. McAvoy JW. Cell division, cell elongation and the coordination of crystallin gene expression during lens morphogenesis in the rat. *J Embryol Exp Morphol*. 1978;45:271–281.
50. Sikic H, Shi Y, Lubura S, Bassnett S. A full lifespan model of vertebrate lens growth. *R Soc Open Sci*. 2017;4:160695.
51. Taiyab A, Holms J, West-Mays JA. β-Catenin/Smad3 interaction regulates transforming growth factor-β-induced epithelial to mesenchymal transition in the lens. *Int J Mol Sci*. 2019;20:2078.
52. Shu DY, Wojciechowski M, Lovicu FJ. ERK1/2-mediated EGFR-signaling is required for TGFβ-induced lens epithelial-mesenchymal transition. *Exp Eye Res*. 2019;178:108–121.
53. Menko AS, Bleaken BM, Libowitz AA, Zhang L, Stepp MA, Walker JL. A central role for vimentin in regulating repair function during healing of the lens epithelium. *Mol Biol Cell*. 2014;25:776–790.
54. Uribe-Querol E, Rosales C. Phagocytosis: our current understanding of a universal biological process. *Front Immunol*. 2020;11:1066.
55. Gordon S. Phagocytosis: an immunobiologic process. *Immunity*. 2016;44:463–475.
56. Garcia-Porrero JA, Colvee E, Ojeda JL. The mechanisms of cell death and phagocytosis in the early chick lens morphogenesis: a scanning electron microscopy and cytochemical approach. *Anat Rec*. 1984;208:123–136.
57. Galichanin K, Lofgren S, Bergmanson J, Soderberg P. Evolution of damage in the lens after in vivo close to threshold exposure to UV-B radiation: cytomorphological study of apoptosis. *Exp Eye Res*. 2010;91:369–377.
58. Ishizaki Y, Voyvodic JT, Burne JF, Raff MC. Control of lens epithelial cell survival. *J Cell Biol*. 1993;121:899–908.
59. Feeney-Burns L, Burns RP, Anderson RS. Ultrastructure and acid phosphatase activity in hereditary cataracts of deer mice. *Invest Ophthalmol Vis Sci*. 1980;19:777–788.
60. Smith JW, Vestal DJ, Irwin SV, Burke TA, Cheresh DA. Purification and functional characterization of integrin alpha v beta 5. An adhesion receptor for vitronectin. *J Biol Chem*. 1990;265:11008–11013.
61. Leifheit-Nestler M, Conrad G, Heida NM, et al. Overexpression of integrin beta 5 enhances the paracrine properties of circulating angiogenic cells via Src kinase-mediated activation of STAT3. *Arterioscler Thromb Vasc Biol*. 2010;30:1398–1406.
62. Lakkaraju A, Umapathy A, Tan LX, et al. The cell biology of the retinal pigment epithelium. *Prog Retin Eye Res*. 2020;78:100846.
63. Shui YB, Sasaki H, Pan JH, et al. Morphological observation on cell death and phagocytosis induced by ultraviolet irradiation in a cultured human lens epithelial cell line. *Exp Eye Res*. 2000;71:609–618.
64. Memmo LM, McKeown-Longo P. The alphavbeta5 integrin functions as an endocytic receptor for vitronectin. *J Cell Sci*. 1998;111(Pt 4):425–433.
65. Taliana L, Evans MD, Ang S, McAvoy JW. Vitronectin is present in epithelial cells of the intact lens and promotes epithelial mesenchymal transition in lens epithelial explants. *Mol Vis*. 2006;12:1233–1242.
66. Lin H, Ouyang H, Zhu J, et al. Lens regeneration using endogenous stem cells with gain of visual function. *Nature*. 2016;531:323–328.
67. Zukin LM, Pedler MG, Chyung K, et al. Aldose reductase inhibition enhances lens regeneration in mice. *Chem Biol Interact*. 2019;307:58–62.
68. Liu Z, Wang R, Lin H, Liu Y. Lens regeneration in humans: using regenerative potential for tissue repairing. *Ann Transl Med*. 2020;8:1544.
69. Vergara MN, Tsissios G, Del Rio-Tsonis K. Lens regeneration: a historical perspective. *Int J Dev Biol*. 2018;62:351–361.

Investigative Ophthalmology & Visual Science